Optical trapping of metal-dielectric nanoparticle clusters near photonic crystal microcavities

Camilo A. Mejia,[1,*] Ningfeng Huang,[2] and Michelle L. Povinelli[2]

[1]*Department of Physics and Astronomy, University of Southern California, Los Angeles, California 90089, USA*

[2]*Ming Hsieh Department of Electrical Engineering, University of Southern California, Los Angeles, California 90089, USA*

**Corresponding author: mejiapra@usc.edu*

Received July 17, 2012; accepted July 29, 2012;
posted August 3, 2012 (Doc. ID 172743); published August 29, 2012

We predict the formation of optically trapped, metal-dielectric nanoparticle clusters above photonic crystal microcavities. We determine the conditions on particle size and position for a gold particle to be trapped above the microcavity. We then show that strong field redistribution and enhancement near the trapped gold nanoparticle results in secondary trapping sites for a pair of dielectric nanoparticles. © 2012 Optical Society of America

OCIS codes: 350.4855, 050.5298, 250.5403.

Recent research has explored the use of strong electromagnetic field gradients near microphotonic structures for optical trapping and manipulation [1–7]. In particular, photonic-crystal microcavities have been designed for use as localized particle traps [8–11]. For a small, dielectric particle, the trapping of a particle near a microcavity can be viewed in terms of the interaction of the induced dipole in the particle with the electric field.

Metallic particles are also subject to light forces [12–17]. Unlike dielectric nanoparticles, metal particles can significantly redistribute the electromagnetic fields in their vicinity, enhancing the field strength near their surfaces. In this work, we propose to exploit the field redistribution near a trapped metallic particle to form metallo-dielectric nanoparticle clusters with well-defined morphologies. In particular, we use a photonic crystal microcavity to form an optical trap for a gold nanoparticle. We then show that field enhancement near the nanoparticle forms secondary trapping sites for a pair of dielectric nanoparticles.

We consider the photonic crystal microcavity shown in Fig. 1(a). The photonic crystal is formed of a hexagonal lattice of holes in Si ($n = 3.46$). The lattice constant is 400 nm, the hole radius is 140 nm, and the thickness of the silicon slab is 200 nm. The microcavity is created by removing a hole and displacing its two nearest neighbors along the x direction outward by 8 nm [8]. The photonic crystal rests on a SiO_2 substrate ($n = 1.45$), and the holes in the lattice and the region above the crystal are filled with water ($n = 1.33$).

The microcavity mode was simulated using the finite-difference time-domain (FDTD) method. A y-polarized plane wave illuminates the microcavity from below. We take the computational cell to be $3.6\ \mu m \times 3.4\ \mu m \times 2\ \mu m$ in size. PML boundary conditions were used. A microcavity resonance value of 226.9 THz and quality factor $Q \sim 60$ were obtained. The microcavity strongly enhances the electric field near the missing hole, and the field intensity is 80 times higher than without the microcavity in the midplane of the slab. The intensity decays by a factor of 30 at a height of 130 nm above the slab. At this height, we have observed that the strongest local intensity is achieved slightly off resonance ($f = 229.1$ THz. The field intensity in $(V/m)^2$ is plotted in Fig. 1(b) for a source power of $1.84\ mW/\mu m^2$.

We calculate the optical force from the Maxwell Stress Tensor. In Fig. 2, we plot the normalized optical force in the vertical direction for gold nanoparticles with several different radii. The bottom edge of each particle is 50 nm above the surface of the slab, and each particle is centered on the microcavity. F_z is the z-component of the optical force, c is the speed of light in vacuum, and the flux is the total electromagnetic flux over the computational cell. A negative force indicates attraction toward the microcavity, whereas a positive force indicates repulsion. We observe both strong size and frequency dependence of the optical force near the microcavity resonance. For the largest gold particle shown ($r = 160$ nm), the force exhibits a Fano-resonance-like shape and is repulsive (positive force). For the smallest gold particle shown ($r = 80$ nm), the force exhibits a single dip and is attractive (negative force). The force on an 80 nm gold particle is an order of magnitude larger than that felt by a dielectric particle of the same size. For particles of intermediate sizes, the force transforms from a Fano shape to a single dip. Thus, only gold particles with radii smaller than 160 nm can be trapped.

Qualitatively, we can understand the different shapes of the curves in Fig. 2 using insight from the dipole approximation [17]. For trapping to occur, the attractive gradient force must be larger than the sum of the repulsive scattering and absorption forces. From the analytical expressions in [17], it can easily be shown that the gradient force on a gold particle is attractive and has the form of a single dip near resonance, while the scattering

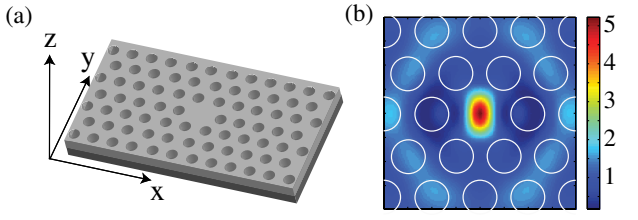

Fig. 1. (Color online) (a) Photonic crystal microcavity. (b) Electric field intensity above the slab slightly off resonance.

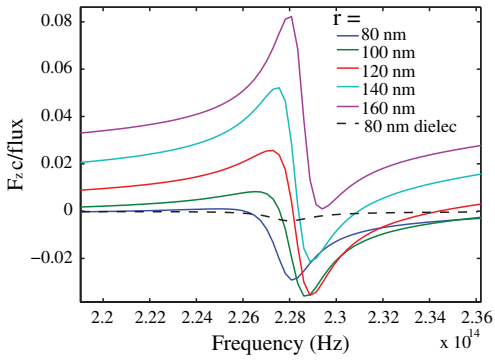

Fig. 2. (Color online) Vertical force on gold nanoparticles of different sizes and a dielectric particle with $r = 80$ nm and $\varepsilon = 1.59$.

and absorption forces are repulsive and have a Fano-like shape.

Looking at Fig. 2, we observe that for small particles (e.g., $r = 80$ nm), the shape of the optical force curve resembles that of a gradient force term. For larger particles (e.g., $r = 160$ nm), the shape of the curve resembles that of scattering and absorption terms. We infer that as the particle size decreases, the gradient force dominates the scattering and absorption effects, leading to trapping.

In Fig. 3(a), we plot the frequency-dependent vertical force on a gold particle with $r = 80$ nm for several different heights, assuming the particle is centered over the microcavity. The frequency at which the optical force peaks shifts as a function of particle height, due to the interaction between the gold particle and the microcavity. This effect is similar to the self-induced trapping effect previously observed for dielectric particles [8]. For a frequency of 229.1 THz, the force is attractive for all heights shown.

We fix the excitation frequency at 229.1 THz and consider the spatial dependence of the optical force. In Figs. 3(b) and 3(c), we show the normalized horizontal and vertical forces (Fc/flux) on a gold particle whose bottom edge is located 50 nm above the slab. The color bars indicate the magnitude, and the arrows in Fig. 3(b) indicate the direction. There is a stable trapping position

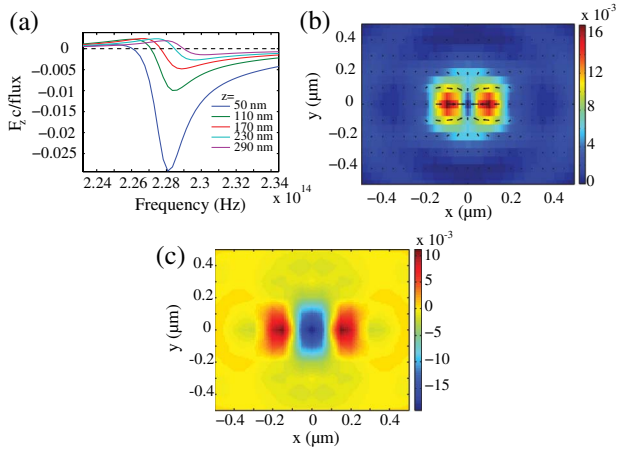

Fig. 3. (Color online) (a) Vertical force as a function of frequency for several different vertical positions. Normalized force in the (b) horizontal and (c) vertical directions as a function of position in the x-y plane for a gold particle with $r = 80$ nm.

at the center of the microcavity. The trap is weakest along the y-direction and has a stiffness [10] $k_y = 0.2\ \mathrm{pN\,nm^{-1}\,W^{-1}}$. We estimate a minimum trapping power of 1 mW by requiring the stability number to be at least 1 [2].

A gold nanoparticle trapped at the center of the microcavity will redistribute the electromagnetic field, forming new optical trapping locations. Figures 4(a) and 4(b) show the electric field intensity 130 nm above the slab at the fixed frequency of 229.1 THz for the same source power as in Fig. 1. The maximum value of intensity is 7 times higher than without a gold particle. The high intensity regions can attract dielectric particles. Figures 4(c) and 4(d) show the horizontal and vertical optical forces on a dielectric particle with $n = 1.59$ and $r = 80$ nm in the presence of the trapped gold nanoparticle, indicated by the solid, yellow circle. The dielectric particle is stably trapped in the position indicated by the dashed circles. In the figures, the arrows next to the graphs represent values of Fc/flux $= 0.002$. We estimate a minimum trapping power of 7 mW with trapping stiffnesses of $k_x = 0.08\ \mathrm{pN\,nm^{-1}\,W^{-1}}$, $k_y = 0.25\ \mathrm{pN\,nm^{-1}\,W^{-1}}$ and $k_z = 0.09\ \mathrm{pN\,nm^{-1}\,W^{-1}}$.

By symmetry, a second possible trapping position exists on the opposite side of the gold particle. Figure 4(e) shows the optical force on a dielectric particle with $r = 80$ nm after both a gold and dielectric particle are trapped in the locations shown by the solid yellow and blue circles, respectively. The arrow next to the graph represents a value of Fc/flux $= 0.002$. The dielectric particle is trapped in the position indicated by the dashed line. The results of Fig. 4 thus indicate that dielectric-metal-dielectric clusters will be formed, consisting of three particles with composition and orientation as shown.

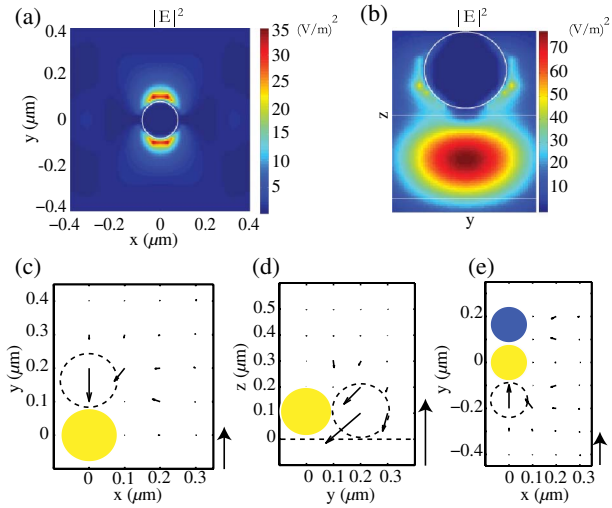

Fig. 4. (Color online) Electric field intensity in the midplane (a) and on a vertical cut (b) of a trapped gold particle with $r = 80$ nm. Horizontal (c) and vertical (d) optical forces as a function of position for a dielectric particle with $r = 80$ nm in the presence of a trapped gold particle (yellow circle); (e) Horizontal optical force as a function of position for a dielectric particle near trapped gold (yellow) and dielectric (blue) particles. The arrows next to the graph represent Fc/flux $= 0.002$.

We note that the specific force values and the required power for trapping calculated here assume normally incident light distributed over an area of approximately 12 μm^2. In an experiment, the coupling efficiency between the incident light and the cavity can likely be increased by adjusting the spot size of the normally incident beam and/or using a side-coupled waveguide to inject light into the microcavity mode, increasing the optical forces and reducing the power required for trapping.

In an experiment, surface treatment of the gold nanoparticles, dielectric nanoparticles, and photonic crystal may be required to prevent aggregation, adhesion, and/or electrostatic effects. Previous experimental work in the literature has developed techniques for preventing aggregation of gold [14] and dielectric [5] nanoparticles, as well as adhesion between nanoparticles and microphotonic devices [10]. Electrostatic interactions in the system can be minimized using a phosphate buffer solution with a regulated pH of 7.0 [18].

We simulated the heating-induced fluid convection in COMSOL and used Stoke's law to estimate the drag force exerted on particles by flow in a 10 μm thick channel. The heating source in the simulation is calculated using the spatially dependent electric fields obtained from FDTD simulations. For an incident power of 10 mW, the maximum temperature rise is ~7 K, and the maximum flow speed is ~0.1 nm/s. The normalized drag force $F_d c$/flux on a 80 nm radius gold particle is estimated to be less than 4×10^{-9}, which is negligible compared to the optical trapping force.

In summary, we have proposed a method for using optical forces to induce the formation of metallo-dielectric clusters with controlled morphology. The method relies on field-enhancement effects near gold particles trapped above a photonic-crystal microcavity. If the self-assembly process is performed in a photopolymerizable solution, a secondary laser spot could be used to locally solidify the region around the cluster. Moreover, integration with a microfluidic channel could allow for controlled, sequential delivery of individual gold and metal particles, along with controlled collection of metallo-dielectric clusters.

This work is funded by an Army Research Office Young Investigator Award under award No. 56801-MS-PCS. Computation resources were provided by USC HPCC (www.usc.edu/hpcc).

References

1. K. Okamoto and S. Kawata, Phys. Rev. Lett. **83**, 4534 (1999).
2. A. H. J. Yang and D. Erickson, Nanotechnology **19**, 045704 (2008).
3. A. H. J. Yang, S. D. Moore, B. S. Schmidt, M. Klug, M. Lipson, and D. Erickson, Nature **457**, 71 (2009).
4. A. N. Grigorenko, N. W. Roberts, M. R. Dickinson, and Y. Zhang, Nature Photon. **2**, 365 (2008).
5. M. L. Juan, R. Gordon, Y. Pang, F. Eftekhari, and R. Quidant, Nat. Phys. **5**, 915 (2009).
6. M. Righini, G. Volpe, C. Girard, D. Petrov, and R. Quidant, Phys. Rev. Lett. **100**, 186804 (2008).
7. C. A. Mejia, A. Dutt, and M. L. Povinelli, Opt. Express **19**, 11422 (2011).
8. M. Barth and O. Benson, Appl. Phys. Lett. **89**, 253114 (2006).
9. A. Rahmani and P. C. Chaumet, Opt. Express **14**, 6353 (2006).
10. S. Mandal, X. Serey, and D. Erickson, Nano Lett. **10**, 99 (2010).
11. J. Hu, S. Lin, L. C. Kimerling, and K. Crozier, Phys. Rev. A. **82**, 053819 (2010).
12. J. R. Arias-Gonzalez and M. Nieto-Vesperinas, J. Opt. Soc. Am. A **20**, 1201 (2003).
13. F. Hajizadeh and S. N. S. Reihani, Opt. Express **18**, 551 (2010).
14. L. Bosanac, T. Aabo, P. M. Bendix, and L. B. Oddershede, Nano Lett. **8**, 1486 (2008).
15. K. Wang, E. Schonbrun, and K. B. Crozier, Nano Lett. **9**, 2623 (2009).
16. A. S. Zelenina, R. Quidant, and M. Nieto-Vesperinas, Opt. Lett. **32**, 1156 (2007).
17. K. Svoboda and S. M. Block, Opt. Lett. **19**, 930 (1994).
18. B. S. Schmidt, A. H. J. Yang, D. Erickson, and M. Lipson, Opt. Express **15**, 14322 (2007).